HHS Public Access

Author manuscript

Cancer Immunol Res. Author manuscript; available in PMC 2020 June 01.

Published in final edited form as:

Cancer Immunol Res. 2019 June ; 7(6): 896–909. doi:10.1158/2326-6066.CIR-18-0713.

Function of Human Tumor-Infiltrating Lymphocytes in Early Stage Non-Small Cell Lung Cancer

Shaun M. O'Brien[1,*], **Astero Klampatsa**[1], **Jeffrey C. Thompson**[1], **Marina C. Martinez**[1], **Wei-Ting Hwang**[2], **Abishek S. Rao**[3], **Jason E. Standalick**[3], **Soyeon Kim**[1], **Edward Cantu**[4], **Leslie A. Litzky**[5], **Sunil Singhal**[3], **Evgeniy B. Eruslanov**[3], **Edmund K. Moon**[1], and **Steven M. Albelda**[1]

[1]Division of Pulmonary, Allergy, and Critical Care, Perelman School of Medicine at the University of Pennsylvania, Philadelphia, PA 19104

[2]Department of Biostatistics, Epidemiology and Informatics, Perelman School of Medicine at the University of Pennsylvania, Philadelphia, PA 19104

[3]Division of Thoracic Surgery, Perelman School of Medicine at the University of Pennsylvania, Philadelphia, PA 19104

[4]Division of Cardiovascular Surgery, Perelman School of Medicine at the University of Pennsylvania, Philadelphia, PA 19104

[5]Department of Pathology and Laboratory Medicine, Perelman School of Medicine at the University of Pennsylvania, Philadelphia, PA 19104

Abstract

Cancer progression is marked by dysfunctional tumor-infiltrating lymphocytes (TILs) with high inhibitory receptor (IR) expression. Since inhibitory receptor blockade has led to clinical responses in some non-small cell lung cancer (NSCLC) patients, we investigated how IRs influenced $CD8^+$ TIL function from freshly digested early-stage NSCLC tissues using a killing assay and intracellular cytokine staining after *in vitro* T-cell restimulation. Early-stage lung cancer TIL function was heterogeneous with only about one-third of patients showing decrements in cytokine production and lytic function. TIL hypofunction did not correlate with clinical factors, co-existing immune cells (macrophages, neutrophils, or $CD4^+$ T regulatory cells), nor with PD-1, TIGIT, TIM-3, CD39 or CTLA-4 expression. Instead, we found that the presence of the integrin $\alpha_e\beta_7$ (CD103), characteristic of tissue resident memory cells (T_{RM}), was positively associated with cytokine production, whereas expression of the transcription factor Eomesodermin (Eomes) was negatively associated with TIL function. These data suggest that the functionality of $CD8^+$ TILs from early-stage NSCLCs may be influenced by competition between an antitumor $CD103^+$ T_{RM} program and an exhaustion program marked by Eomes expression. Understanding the mechanisms of T-cell function in the progression of lung cancer may have clinical implications for immunotherapy.

[*]Corresponding author: Shaun O'Brien, shaunobrien81@gmail.com.

Conflict of interest: No conflicts of interest exist

Keywords

Non-Small Cell Lung Cancer; Tissue Resident Memory Cells; Eomes; Checkpoint Inhibitors; $CD8^+$ TILs

Introduction

Non-small cell lung cancer (NSCLC) is a lethal cancer. However, inhibitory receptor (IR) blockade, specifically with PD-1 and PD-L1 antibodies, has demonstrated antitumor efficacy in a subpopulation of advanced NSCLC patients (1). Successful anti-PD1 therapy has triggered interest in other potential IRs or actionable immune targets on tumor-infiltrating lymphocytes (TILs). IRs identified on NSCLC TIL subsets include Cytotoxic T-Lymphocyte-Associated protein-4 (CTLA-4), T-cell Immunoglobulin and Mucin-domain containing-3 (TIM-3), CD39, and T-cell Immunoreceptor with Ig and ITIM domains (TIGIT) (2–6). The integrin $\alpha_E\beta_7$ (known as CD103), which marks tissue resident memory cells (T_{RM}s), is expressed on lung cancer TILs and is positively correlated with clinical outcome (7–9).

Despite this increasingly detailed insight into the immune phenotype of NSCLC TILs, relatively little work has focused on the interplay of specific surface receptors and TIL function. Many of these inhibitory receptors can also be markers of T-cell activation. For example, PD-1 is up-regulated on recently activated $CD8^+$ T cells (10) and marks a set of neo-antigen specific melanoma TILs (11). Tumor T_{RM}'s, which are reactive T cells, also overexpress PD-1 constitutively (7,12,13).

To study early-stage NSCLC TIL function, we performed flow cytometric single cell analyses after suboptimal T-cell receptor (TCR) stimulation. We found that early-stage NSCLC TILs had heterogeneous cytokine production and cytolytic activity, and that function was not correlated with inhibitory receptor expression. However, T-cell function was positively associated with CD103 expression and negatively associated with transcription factor Eomesodermin (Eomes) expression.

Methods

Patient Selection:

The Perelman School of Medicine Institutional Review Board, in accordance with the US Common Rule, approved this study and all patients signed informed consent. Patient samples (from 2014 to 2017) were obtained from: i) 44 early-stage NSCLC (Stage I-III) patients undergoing potentially curative surgery, ii) 8 patients with advanced stage NSCLC (Stage IV) via fine needle aspirates (FNAs), and iii) 5 patients with malignant pleural effusions (MPEs) from advanced NSCLC. Whenever possible, peripheral blood mononuclear cells (PBMC) and uninvolved lung tissue from the same lung lobe (as distal from the tumor as possible) were collected. Healthy appearing lung tissue obtained from 21 non-transplantable organ transplant donors (due to focal areas of pneumonia or donor hypoxemia) were processed. Table 1 presents details.

Tissue Acquisition and Processing:

After resection, tissues, MPE's, and PBMCs were digested within two hours using validated approaches to minimize cell surface marker cleavage (14). For transplant donors, the median time between removal of the lung until tissue processing was 7 hours. All digests and samples were analyzed immediately, without freezing or overnight "rest".

Fine Needle Aspirates:

Late stage NSCLC tumor tissue was obtained via 21g or 22g endobronchial ultrasound transbronchial aspiration needle (15). Samples were flushed into tissue culture media and immediately processed as above.

Immunophenotyping/Flow Cytometry:

After digestion, samples were stained and analyzed using standard flow cytometry approaches. Single cell suspensions from all samples were stained with Live Dead Blue (Invitrogen, 1:400 in PBS) for 10 minutes at 4°C, washed with FACs Buffer (1% FBS in PBS) and then stained with cell surface marker antibodies for 45 minutes, 4°C. For Ki-67 and FoxP3 staining, cells were fixed with eBioscience Fix/Perm for one hour at 4°C, and washed two times with eBioscience Perm/Wash Buffer. Cells were stained in presence of Perm Wash for 45 minutes at 4°C.

Antibodies used were anti-human CD3 (UCHT1, SK7), CD4 (OKT4), CD69 (FN50), CD103 (Ber-Act8), PD-1 (EH12-H7), TIM3 (F38–2E2), CD62L (DREG-56), CD45RO (UCHL1), CD39 (A1), Foxp3 (206D), CD45RA (HI100), PDL-1 (M1H1), CD14 (M5E2), CD15 (HI98) from Biolegend; Anti-human CD8 (RPA-T8), CTLA-4 (BN13), from BD Bioscience; and anti-human TIGIT (MBAS43), Eomes (WD1928) and Ki-67 (20Raj1) from eBiosciences.

Intracellular cytokine staining was performed as detailed previously (16). Cytokine antibodies used were directly conjugated anti-human IFN−γ (4S.B3), TNF-α (MAb11), and IL-2 (MQ1–17H12) from Biolegend. For concurrent transcription factor and cytokine staining, the cells were treated by the eBioscience FoxP3 staining protocol. Flow Cytometric analysis was performed on a BD Fortessa (BD Pharmingen).

Labeled cells were washed and re-suspended in FACs buffer for flow cytometric analysis on a BD Fortessa with FACS Diva Software (BD Biosciences) and analyzed using FlowJo 10.2. Negative gating was based on a "fluorescence minus one" (FMO) strategy. viSNE, a visualization tool of high-dimensional single cell data based on t-Distributed Stochastic Neighbor Embedding (t-SNE) algorithm was generated via FCS Express 6 (De Novo Software).

Functional Assays:

To assess cytokine production, single cell suspensions were placed in RPMI-1640 medium (supplemented with 10% FBS, L-glutamine, Penicillin, Streptomycin, 2-βME) with GolgiStop (BD Biosciences, 0.66ul/ml) and GolgiPlug (BD Biosciences, 1ul/ml) followed by stimulations in media alone, PMA (30ng/ml) and Ionomycin (1uM) (PMA/I), or 0.5ug/ml

plate-bound anti-human CD3 (OKT3, Biolegend). After 37°C overnight stimulation, cells were harvested and stained for surface markers as described above. Intracellular cytokine staining was performed as detailed previously (16).

Bispecific T cell engager (BiTE) killing assay: To measure cytotoxicity, we employed a BiTE killing assay similar to that recently reported (4). A lentiviral expression vector (17) (graciously provided by Dr. Yang Bing Zhao, UPenn) was constructed to produce a BiTE by fusing the scFV from blinitumamab (that recognizes CD3) with the scFV from SS1 that recognizes mesothelin. 293 cells were transduced by the vector and supernatant was collected. We also generated a human mesothelioma cell line that expressed high levels of mesothelin and luciferase (EMMESO) (18). The killing assay was performed by plating EMMESO target tumor cells at 5000/well in a 96 well plate and allowing them to adhere over a 4–6hour period. A volume of digested patient tumor cell suspension was then added to the EMMESO cells based on live CD8+ T cells frequency (as measured by flow cytometry) to achieve a ratio of ~10 CD8+ T cells to 1 EMMESO tumor cell. 30 μl of BiTE supernatant or control media was added to some wells of those cocultures. After 18 hours of coculture, the supernatant from the wells was aspirated, the remaining tumor cells were washed and then lysed. Luminescence from the remaining tumor cells was measured using a Glomax Luminometer (Promega, Inc). Percent lysis was measured using the formula % killing = 100 – [(luminescence of tumor alone well – luminescence of cocultured well) / (luminescence of tumor alone well) × 100]. BiTE-induced killing was the difference in % lysis measured in BiTE + digest + tumor wells and digest + tumor wells. As a control, we used the EMParental cell line (a mesothelin-negative mesothelioma cell line).

Statistical Analysis:

Descriptive statistics were computed for all variables. Because most of our data did not deviate from a normal distribution (using Shapiro-Wilk test and histograms), parametric tests were applied. Comparison between two independent samples was based on two-sample t-test or paired t-tests when appropriate. One-Way ANOVA was used to compare multiple groups, followed by ad-hoc pairwise comparison using Tukey's correction if the overall F-test was significant. Pearson's Chi-Squared test was used to compare hypofunction proportions between independent groups of patients or McNear test for paired samples. All tests were two-sided, $p<0.05$ was considered statistically significant.

Heat Map Data: Data (non-log transformed) was visualized in a heat map format using the Morpheus software (https://software.broadinstitute.org/morpheus/).

Results

Patient and sample characteristics

We studied T-cell function from (i) tumor-free lung lymphocytes (TFLLs), (ii) lung tissue adjacent to resected lung cancers (distant lung-associated lymphocytes or DLALs), (iii) tumor-infiltrating lymphocytes from early-stage resected lung cancers (TILs), (iv) malignant pleural effusions (MPEs) from Stage IV NSCLC patients, and (v) TILs from advanced stage

lung cancers obtained by fine needle aspirates (FNAs) (see Methods). Selected patient characteristics are summarized in Table 1.

Early-stage lung cancer TIL heterogeneity

To test $CD8^+$ T-cell baseline function, we cultured tissue digests overnight with monensin and brefeldin and performed intracellular cytokine staining. The $CD8^+$ TFLLs, DLALs, and TILs showed little spontaneous intracellular IFNγ production (Supplementary Fig. S1A) consistent with previous reports (5).

We thus designed an assay to stimulate cytokine secretion by sub-optimal TCR stimulation determined by titration of plate-bound anti-CD3 using a dose of 0.5 ug/ml (Supplementary Fig. S1B). To control for intra-assay variability with non-batched patient samples, to prove the cells were capable of activation, and to interrogate distal TCR signaling, we also stimulated the T cells overnight with PMA/I. This resulted in robust IFNγ production with 85–88% of $CD8^+$ cells making cytokine (Supplementary Fig. S1C). We confirmed that TCR stimulation with overnight monensin and brefeldin did not alter inhibitory receptor surface expression (Supplementary Fig. S2). We only analyzed freshly processed samples, as thawing of cryopreserved tumor digests resulted in increased TIL function (Supplementary Fig. S3A).

Using this TCR-stimulation assay, we found an average of 33.4% of the $CD8^+$ TFLLs produced IFNγ (Fig. 1A) and a similar percentage (36%) by the $CD8^+$ DLALS. However, the TILs were significantly less functional ($p<0.05$), with an average of 25.3% of $CD8^+$ T cells producing IFNγ. The percentage of cells producing IFN-γ and TNF-α (Fig. 1B) in the TILs was concordant (Spearman's Rho=0.69; $p<0.0001$). $IFN\gamma^+TNF\alpha^+IL2^+$ frequencies were also similar among the tissue digests (Supplementary Fig. S3B–3C). We therefore used IFNγ as our primary cytokine readout.

For analytic purposes, we defined T cells as hypofunctional if the percentage of IFNγ-secreting $CD8^+$ T cells was less than one standard deviation from the TFLL mean (<19.3%) and confirmed that TFLL function was not influenced by ischemia time (Supplementary Fig. S4A). Using this definition, hypofunctional $CD8^+$ T cells constituted 19% (4/21) in TFLLs, 20% (9/44) in DLALs and 36% (16/44) in TILs, with statistically significant differences between the DLALs and TILs ($p=0.03$).

Because the hypofunctional TIL frequency was low in early-stage patients, we examined TILs obtained from 8 advanced lung cancer cases and from 5 malignant lung cancer effusions. The late stage TIL and MPE samples (Fig. 1A) were more hypofunctional, making significantly ($p=0.01$) less IFNγ than the early-stage patients.

We also tested a subset of TIL digests (n=14) for cytolytic activity using a bispecific antibody assay (see Methods) (Fig. 1C). Under our experimental conditions, the average lytic activity by hypofunctional TILs was 13%, which was significantly lower ($p=0.02$) than in functional TIL digests (23.8%).

TIL functional heterogeneity is not associated with clinical factors

Since only about one third of the early-stage NSCLC patients had hypofunctional T-cell function, we could examine clinical factors that were potentially associated with functionality. Using our 19.3% cutoff to define hypofunction, we found that patient gender, smoking history, histology, tumor stage, age, and tumor size had little influence on $CD8^+$ TIL function (Supplementary Fig. S4B–G). However, using correlation analyses, we observed trends towards hypofunction in patients who were older (p=0.08) or with larger tumors (p=0.14) (Supplementary Fig. S4H and I).

We also studied the relationship of T-cell function with the tumor mutational status. In the 29 patients with available data, 9 (31%) had *EGFR* mutations, 8 (28%) had *KRAS* mutations, and 16 (55%) had p53 mutations. 75% of patients with *KRAS* mutations also had p53 mutations and none had concomitant *STK11* mutations. We calculated the percentage of IFNγ secreting cells for each mutation (Supplementary Table S1A) and found that patients with *KRAS* mutations had more functional T cells than those with wild-type *KRAS* *(p<0.05)*.

TIL functional heterogeneity not associated with other cell

TILs contained a significantly higher frequency of $FoxP3^+CD4^+$ Tregs (10.5%) in comparison to TFLLs (2.2%), DLALs (3.4%), and PBMCs (3%) (p<0.0001) (Fig. 2A, **left panel**). However, the $CD4^+$ Treg percentages in the functional vs hypofunctional patients were not significantly different (Fig. 2A, **right panel**).

In a subset of patients, we characterized frequencies of $CD14^+$ myeloid cells (tissue monocytes and macrophages) and $CD15^+$ cells (neutrophils) (Fig. 2B and 2C). We observed similar frequencies in all tissue types and no differences between functional and hypofunctional cases. We also performed correlation analyses for tumor microenvironment (TME)-associated cell types (Supplementary Fig. S5A–C) and saw no significant relationships with tumor digest IFN-γ production.

TIL functional heterogeneity correlates with $CD8^+$ *TIL proliferation*

As shown in Fig. 2D (left panel), the $CD8^+$ cell frequency was lowest in TFLLs (mean 5.8%), intermediate in the tumors (mean 11.9%), and highest in distant lung tissue (15.2%). Each group was statistically different (p<0.05) from the other. $CD8^+$ TIL frequency was not different between functional and hypofunctional cases (Fig. 2D, **right panel;** Supplementary Fig. S5D).

We characterized $CD8^+$ T-cell proliferation (Ki-67%) and observed that $CD8^+$ TILs had significantly more proliferation (26%) compared to PBMCS (5.4%), TFLLs (6.5%), and the DLALs (9.5%) Fig. 2E, **left panel**). The functional cases had significantly increased Ki-67 activity versus the hypofunctional cases (30% vs 12%, p=0.002) (Fig. 2E, **right panel;** Supplementary Fig. S5E).

TIL functional heterogeneity is not associated with differentiation status.

The differentiation status of $CD8^+$ TFLLs, DLALs, and TILs was similar, each consisting primarily of effector memory T cells ($CD45RO^+CD62L^-$) (mean 58%−70.4%) and effector cells ($CD45RO^-CD62L^-$) (mean 18.2%−30.3%) (Fig. 2F–G). TIL effector and effector memory $CD8^+$ T-cell frequencies had little influence on TIL functional status (Fig. 2H; Supplementary Fig. S5F–G). In comparison, PBMCs showed more naïve cells and fewer memory T cells (all p values <0.0001 Supplementary Fig. S6A–H). We also determined that TIL $CD8^+RO^-$ cells (mostly effector cells) and $CD8^+RO^+$ cells (mostly effector memory T cells) had similar IFNγ production (Supplementary Fig. S6I).

Heterogeneous expression of inhibitory receptors on tissue lymphocytes and PBMC

With regard to T cell IR expression, we observed minimal Lag3 and BTLA. In contrast, PD-1 expression was high, but very heterogeneous, being expressed significantly more on $CD8^+$ TILs (57.9%), TFLLs (66.6%), and DLALs (42%) compared to PBMCs (21.3%) (all p<0.001) (Fig. 3A, **left and middle panel).**

Tumor PDL-1 assessment in a subset of patients (Fig. 3B, **left panel**) revealed that PDL-1 expression on $CD3^-$ cells (tumor cells and macrophages) was relatively low in the DLALs (11%) and TILs (15.8%). PDL-1 expression did not differ between functional and hypofunctional patient cohorts (Fig. 3B. **right panel,** Supplementary Fig. S7A).

The inhibitory receptor TIGIT was highly expressed on DLALs (55.4%), TILs (61%), and PBMCs (54%), but significantly less expressed on the TFLLs (33.4%) (p<0.001) (Fig. 3C). TIM-3 expression was highest on TILs (16.4%) in comparison to DLALs (8.8%), and PBMC (7.9%), with the TFLLs showing significantly less expression (3.7%) than TILs (p<0.01) (Fig. 3D). The TILs expressed significantly more TIM-3 than the DLALs (P<0.001).

CD39 expression was significantly (p<0.0001) higher on TILs than the other groups (Fig. 3E) similar to other reports (6,8,19). Intracellular CTLA-4 expression was low on TFLLs (13.6%), DLALs (10.5%), and PBMCs (1.9%), with significantly higher expression on the TILs (37.4%) (p<0.001 compared to DLALs and PBMC and p<0.01 compared to TFLLs) (Fig. 3F).

TIL hypofunction not correlated with expression of inhibitory receptors on $CD8^+$ *TILs*

To assess the association between IR expression and overall T-cell function, we plotted from each individual patient their respective percentage of $CD8^+$ T cells expressing IFNγ against their specific IR^+ $CD8^+$ frequency in heatmap format (Fig. 4A). The percentage of IRs on $CD8^+$ TILs from functional versus hypofunctional cases were compared (Fig. 4B). We observed no associations in the heatmap and no statistically significant differences in PD-1, TIGIT, CD39, TIM-3 and iCTLA-4 expression among the functional vs hypofunctional patients. Combined PD-1 expression with other IRs (TIGIT, TIM3, or CTLA-4) also had no influence on TIL function (Fig. 4C). Correlation analyses detailed no significant associations with IR frequency and percent of patient's TILs making IFNγ (Supplementary Fig. S7B–F).

Utilizing intracellular cytokine-based flow cytometry, we measured IFNγ production by specific $CD8^+$ IR^+ TIL population for each patient. As examples, in Fig. 4D, the expression of IFNγ (x axis) is plotted versus the expression of PD-1 (y axis) from two patients' $CD8^+$ TILs. The boxes represent the frequency of $PD1^+$ or $PD1^-$ cells that produced IFNγ. In Patient LC393, the $PD\text{-}1^+$ cells (top quadrants) made more IFNγ in comparison to the $PD\text{-}1^-$ cells (bottom quadrants), whereas in Patient 354, $PD\text{-}1^+$ and $PD\text{-}1^-$ cells made similar amounts of IFNγ. Examples of TIGIT, TIM-3 and CD39 expression vs IFNγ production are shown in Fig. 4E.

The cumulative results of this single cell analysis (Fig. 4F) show considerable heterogeneity, but no significant association of individual or combination of IR expression with IFNγ production. That is, on average, TILs lacking IR expression (IRs= "zero") made similar amounts of IFNγ as those expressing any single or multiple IR combination.

$CD103^+CD45RO^+$ $CD8^+$ T cells are the main source of IFNγ in TILs

Multiple reports have suggested that NSCLC patients with higher $CD8^+$ tissue resident memory cells ($CD103^+CD69^+$) had a better prognosis (7,9,20). We observed high concordance for CD103 and CD69 expression (21) in our patient TILs (Supplementary Fig. S7G) and thus used CD103 as our T_{RM} marker. Our data showed a significantly higher frequency of $CD103^+CD45RO^+CD8^+$ TILs (60.2%) (Fig. 5A, **Top and right panels)** in comparison to TFLLs (36.8%, p=0.006), and DLALs (48.7%, p=0.0015) and neglible expression in PBMCs. When arranged by increasing $CD8^+$ TIL frequency in a heatmap format (Fig. 5A, **lower left panel**), the tumor $CD103^+$ T_{RM} cells were enriched with high $CD8^+$ TIL density, consistent with another report (7). T_{RM} cells have been reported to have high IR expression (7–9,12) and we also noted significantly higher expression of CD39, iCTLA-4, TIM-3, and PD-1 on $CD103^+$ compared with $CD103^-$ $CD8^+$ TILs (Figs. 5A, **lower panel, and** 5B).

Despite increased IR expression, T_{RM}s are reported to be highly reactive cells (7, 12, 22). We therefore assessed if their presence contributed to the IFNγ heterogeneity. Patients with functional TILs had more $CD103^+$ $CD8^+$ cells than the hypofunctional cases (Fig. 5C, 60% vs 38%, n=27, p<0.01) and there was a positive correlation (p=0.05) between the percentage of T_{RM}s and IFNγ production (Supplementary Fig. S7H). At the single cell level, the $CD103^+$ $CD8^+$ TILs had increased IFNγ (Fig 5D) and proliferation (Fig. 5E) in comparison to $CD103^-$ $CD8^+$ TILs. The $CD8^+$ $CD103^+$ cells produced more IFNγ than $CD103^-$ TILs despite similar IR expression (Fig. 5F). Thus, $CD103^+$ TIL expression was a better predictor of functional T cells than IR expression.

Eomes expression in $CD103^+$ T_{RM} cells is associated with loss of TIL function

Despite the $CD103^+$ TILs being a primary IFNγ source in the tumor, this IFNγ production varied (Fig. 5D and F), suggesting additional factors might influence this heterogeneity. Expression of the transcription factor Eomesodermin (Eomes) is associated with exhausted T cells (23–28), and our intracellular flow cytometric assessment of Eomes revealed high expression in the CD8+ TILs, with a significant negative correlation (r^2=0.67, p<0.0001) to

IFNγ production (Fig. 6A). Functional TILs had a significantly lower Eomes expression (43.4%) than hypofunctional TILs (66.7%, $p<0.001$) (Fig. 6B).

T_{RM} cells from normal tissues have low Eomes expression (12,13). We therefore focused on Eomes in the TIL T_{RM} cells. Increased Eomes expression was observed in the $CD103^+$ T_{RM} cells of hypofunctional cases (right panel, Fig. 6C) compared to functional TILs (Fig. 6C, left panel). The percent of patients whose $CD103^+$ TILs expressed Eomes was significantly negatively correlated ($r^2= 0.52$, $p<0.0001$) to overall IFNγ production (Fig. 6D). Patients with functional TILs had a significantly lower percentage of Eomes expression in the $CD103^+$ cells (31.7%) than in hypofunctional TILs (59%, $p<0.001$) (Fig. 6E). Using single cell analysis (Fig. 6F), we observed that $CD103^+Eomes^-$ $CD8^+$ TILs produced significantly ($p<0.05$) more cytokine than $CD103^+Eomes^+$, $CD103^-Eomes^+$, and $CD103^-Eomes^-CD8^+$ T cells. Thus, $CD103^+$ T_{RM} cell hypofunction in early NSCLC tumors was associated with Eomes expression.

To further explore the associations of CD103, Eomes, and IRs with $CD8^+$ TIL function, we applied viSNE analysis (29) to functional TIL case (Fig. 6G–K). After generating a 2D map of $CD8^+$ T cell regions (Fig. 6G), we then applied a heatmap to determine IFNγ and TNFα enriched regions. We identified the regions that did (red circle) or did not (blue circle) produce cytokines (Fig. 6H). $CD103^+$ cells almost exclusively co-localized with cytokine-producing cells (Fig. 6I). The cytokine-enriched region (red circle) expressed little Eomes in comparison to the cytokine negative area (blue circle) (Fig. 6J). One $Eomes^+$ node in the $CD103^+$ region overlapped with the non-cytokine producing region, demonstrating how Eomes abrogates T_{RM} cytokine production. PD-1 analysis (Fig. 6K) showed diffuse expression, consistent with its poor association with cytokine expression and TIL hypofunction.

Discussion

The goal of this study was to evaluate the functional status of early-stage lung cancer TILs primarily by measuring by intracellular cytokine staining by flow cytometry. Since we detected minimal intracellular cytokine production in unstimulated T cells from fresh tumor samples, we submaximally stimulated T cells in fresh tumor digests overnight with a plate-bound anti-CD3 that crosslinks the TCR. Using our assay, we observed that advanced lung cancer TILs were consistently hypofunctional, as might be expected (31–33). In contrast, we found that early-stage lung cancer TIL function was quite heterogeneous and that only about one third of the patients had TILs with hypofunction. Lung TIL function has not been studied extensively, however, functional heterogeneity in early-stage lung cancer TILs after TCR stimulation has been observed by other investigators who measured: (a) cytokine secretion measured by ELISA (3,4), (b) intracellular calcium concentrations (32), and (c) a bispecific antibody (anti-CD3/anti-Folate receptor-alpha) killing assay (4). Our data were consistent with most previous studies with human and mouse TILs in that the defects we observed were in the initial part of the TCR signaling pathway and could be overcome by direct stimulation of the distal part of the signaling pathway by PMA/ionomycin (31,34,35).

The observed TIL functional heterogeneity provided an opportunity to determine what factors were associated with T-cell hypofunction. Function did not correlate with clinical features or with the presence of Tregs, neutrophils, macrophages, or PD-L1 expression. We also saw no correlations of function with $CD8^+$ T-cell numbers or differentiation status. We did note that TILs were more proliferative (as measured by percent Ki-67^+) than other types of lymphocytes and that functionality was associated with increased proliferation.

Given previous studies, we explored the link between hypofunction and expression of IRs that are presumed to define "exhausted" T cells. Our IR expression data was similar to previous reports (2,3,5,7), however the expression of most IRs was not specific to TILs, as we saw a similar phenotype in the lymphocytes from lung tissue adjacent to the tumor and from tumor-free lungs harvested from transplant donors. However, compared to the other lung tissue-resident lymphocytes, TILs expressed more CD39, as observed by others (6,8,19).

Although a hallmark of dysfunctional T cells in tumors is the overexpression of IRs, the actual contribution of these IRs to the dysfunctional state is controversial (33,36,37). Work from some groups (3,4) suggest that the activation and effector function of lung cancer $CD8^+$ TILs correlates with co-expression of multiple immune checkpoints, leading to the suggestion that PD-1^{hi} T cell frequency may be useful as a surrogate marker for TIL functionality upon TCR activation. A report on PD-1^{hi} TILs in NSCLC describes this phenotype (38). In contrast, increasing evidence suggests that IR expression is contextual and may depend just as much on differentiation status as exhaustion in human $CD8^+$ T cells (10,39,40). For example, T_{RM}s, despite being fully functional, express high amounts of PD-1 and other inhibitory receptors (7,8,19). In our study, IR expression on TILs did not seem to predict their functionality. This was true when we compared IR expression on patients with functional versus hypofunctional TILs, as well as when we examined the cytokines secreted by individual $CD8^+$ T cells with or without single or multiple IRs. Our data thus support the idea that using PD-1 as a marker of TIL dysfunction may be misleading; one reason may be because the functional Trm in the tumors express high levels of PD-1.

Trm cells are a subset of effector $CD8^+$ T cells marked by expression of the integrin $\alpha_e\beta_7$ (CD103) and, in lung, the surface marker CD69 (21,41,42). These T_{RM} cells have a genetic program that enables them to react rapidly to potential infectious agents (12, 13) despite expression of IRs (7,8,19). They also express a set of transcription factors that includes high expression of Notch and low expression of Eomes (12). Their presence has been reported as a positive prognostic factor for survival in lung cancer (7,20) and other tumors (8,9). Our data are consistent with these findings. We observed that the $CD103^+$ cells marked more functional TILs that produced more cytokines and proliferated better compared to $CD103^-$ cells, regardless of which IRs were expressed.

In contrast, we observed that expression of the transcription factor eomesodermin (Eomes) was associated with T-cell hypofunction. In murine chronic viral infection models, T-cell exhaustion is characterized by T cells that are $Eomes^{hi}$ and T-Bet^{lo} (23). However, the functions of Eomes and Tbet are complex, interdependent, and likely context dependent

(24,43,44). The actual role of Eomes in driving the exhaustion program thus remains uncertain.

There is relatively little data exploring Eomes function in human T-cell exhaustion, with most of that data obtained from human blood in HIV patients (24,25). A report in NSCLC TILs(28) detailed increased numbers of $Eomes^{hi}T\text{-}Bet^{dim}$ cells, although there were no functional assessments. In our early-stage lung cancer patients, there was a negative correlation (r^2=0.67) between Eomes expression and IFNγ production. Whether Eomes is driving TIL hypofunction or denotes a larger exhaustion program is a question for future research.

Although this study identified TIL functionality within early-stage tumors, it did not address three questions that deserve future study. First, we did not establish the clinical relevance of T-cell function by showing that T-cell hypofunction predicted recurrence rate in these patients. Because of the long observation periods needed to see recurrence, it will take a number of additional years to answer this question. However, we were able to identify 28 patients with at least 2 years of follow up (Supplementary Table S1B). Of these patients, disease has recurred in 9 (32%). The 11 patients with hypofunctional TILs had a recurrence rate of 46%, whereas those 17 patients with functional TILs had a recurrence rate of only 24%, despite the fact that the hypofunctional patients included a higher percentage of Stage 1 patients. The average percentage of TILs making IFNγ was 29.3% in patients without recurrence versus 21% in patients with recurrence. None of these differences are yet statistically significant, but as we have longer follow-up times, a more definitive conclusion can be reached.

Second, we did not attempt to determine which of the TILs were tumor-reactive. Most studies suggest that only a small percentage of TILs recognize tumors (19,45) Reports suggest that these tumor-reactive TILs may be enriched in $CD103^+$ and $CD39^+$ T cell populations (8,19). We did not study the function of $CD103^+CD39^+$ cells, but we saw no increased function in the $CD39^+$ cells vs. $CD39^-$ cells, in contrast to the increased functionality of $CD103^+$ cells.

Third, we did not determine how checkpoint blockade (with anti-PD-1 or anti-PD-L1) related to our findings. We observed that IR expression did not predict T-cell function (exhaustion) after our TCR stimulation assay, however, this assay was performed without testing IR interactions with tumor ligands. In our stimulation assay, we had low endogenous PDL-1 expression on tumors and leukocytes. It is thus possible that we would have seen some additional hypofunction on IR-expressing T cells if these ligands were engaged.

Checkpoint blockade may have its best effects in patients who retain tumor reactive TILs without severe T-cell hypofunction. In mice, these severely hypofunctional cells are proposed to express both high PD-1 (33) and Eomes (23). Our data also suggest that Eomes expression marks a hypofunctional group of human TILs. On the other hand, one study suggests that $PD\text{-}1^{Hi}$ cells might be the most tumor reactive and have the potential for re-invigoration with anti-PD1 therapy (38). To determine which T cells would respond to checkpoint blockade, prospective studies examining markers on TILs (such as CD103,

CD39, and Eomes), as well as TIL functional assays with PD-L1 signals provided in the presence and absence of anti-PD-1, would be needed.

In summary, our findings suggest a model in which early-stage lung cancer TILs are regulated by an antitumoral T_{RM} program competing with a pro-tumoral exhaustion program. Expression of IR ligands could also play a role when the appropriate ligands are present. We speculate that early in tumor formation, circulating effector or effector memory cells encounter antigens within the tumor (perhaps neo-antigens being the most reactive) and are converted to $CD103^+$ T_{RM} cells which then exert some antitumor activity. However, due to a variety of factors associated with tumor growth and the TME, the tumors are not eliminated. These factors, likely in addition to resulting chronic antigen stimulation, then trigger initiation of an exhaustion program characterized by (and possibly driven by) increased Eomes (23) and CD39 expression (8,19). Presence of B7H4 on tumors or other TME cells might function to upregulate Eomes in T cells (46). As the tumors grow, the exhaustion program wins out in the T_{RM} cells, resulting in more and more TILs becoming hypofunctional.

Supplementary Material

Refer to Web version on PubMed Central for supplementary material.

Acknowledgements:

We acknowledge the Donor Lung Acquisition team, Naomi St. Jean, and Mike Annunziata for experimental assistance.

Financial Support: SO was funded by T32-CA009140; AR, MA, JS and EE were funded by DOD-LC140199, W81XWH-15-1-0717, and NIH/NCI CA187392. EC was funded by HL116656 and HL135227. Support was also provided by the Translational Center of Excellence in Lung Cancer Immunology (Abramson Cancer Center) and a grant from Janssen Pharmaceuticals.

References

1. Assi HI, Kamphorst AO, Moukalled NM, Ramalingam SS. Immune checkpoint inhibitors in advanced non-small cell lung cancer. Cancer 2018; 124:248–261. [PubMed: 29211297]
2. Lizotte PH, Ivanova EV, Awad MM, Jones RE, Keogh L, Liu H, et al. Multiparametric profiling of non–small-cell lung cancers reveals distinct immunophenotypes. JCI Insight. 2016;1 e89014. [PubMed: 27699239]
3. Thommen DS, Schreiner J, Muller P, Herzig P, Roller A, Belousov A, et al. Progression of Lung Cancer Is Associated with Increased Dysfunction of T Cells Defined by Coexpression of Multiple Inhibitory Receptors. Cancer Immunology Research. 2015; 3:1344–55. [PubMed: 26253731]
4. Schreiner J, Thommen DS, Herzig P, Bacac M, Klein C, Roller A, et al. Expression of inhibitory receptors on intratumoral T cells modulates the activity of a T cell-bispecific antibody targeting folate receptor. Oncoimmunology. 2015;5:e1062969. [PubMed: 27057429]
5. Tassi E, Grazia G, Vegetti C, Bersani I, Bertolini G, Molla A, et al. Early effector T lymphocytes coexpress multiple inhibitory receptors in primary non-small cell lung cancer. Cancer Res. 2016; 77:851–861. [PubMed: 27979840]
6. Canale FP, Ramello MC, Núñez N, Bossio SN, Piaggio E, Gruppi A, et al. CD39 Expression Defines Cell Exhaustion in Tumor-Infiltrating CD8+ T Cells-Response. Cancer Res. 2018; 78:115–128.

7. Ganesan A-P, Clarke J, Wood O, Garrido-Martin EM, Chee SJ, Mellows T, et al. Tissue-resident memory features are linked to the magnitude of cytotoxic T cell responses in human lung cancer. Nat Immunol. 2017;18:940–950. [PubMed: 28628092]
8. Duhen T, Duhen R, Montler R, Moses J, Moudgil T, de Miranda NF, et al. Co-expression of CD39 and CD103 identifies tumor-reactive CD8 T cells in human solid tumors. Nat Comms. 2018;9:2724.
9. Savas P, Virassamy B, Ye C, Salim A, Mintoff CP, Caramia F, et al. Single-cell profiling of breast cancer T cells reveals a tissue-resident memory subset associated with improved prognosis. Nat Med. 2018;24:986–93. [PubMed: 29942092]
10. Legat A, Speiser DE, Pircher H, Zehn D. Inhibitory receptor expression depends more dominantly on differentiation and activation than "exhaustion" of human CD8 T cells. Frontiers Immunol. 2013; 4:455.
11. Gros A, Robbins PF, Yao X, Li YF, Turcotte S, Tran E, et al. PD-1 identifies the patient-specific CD8+ tumor-reactive repertoire infiltrating human tumors. J Clin Invest. 2014;124:2246–59. [PubMed: 24667641]
12. Hombrink P, Helbig C, Backer RA, Piet B, Oja AE, Stark R, et al. Programs for the persistence, vigilance and control of human CD8(+) lung-resident memory T cells. Nat Immunol. 2016;17:1467–78. [PubMed: 27776108]
13. Mackay LK, Wynne-Jones E, Freestone D, Pellicci DG, Mielke LA, Newman DM, et al. T-box Transcription Factors Combine with the Cytokines TGF-β and IL-15 to Control Tissue-Resident Memory T Cell Fate. Immunity. 2015;43:1101–11. [PubMed: 26682984]
14. Quatromoni JG, Singhal S, Bhojnagarwala P, Hancock WW, Albelda SM, Eruslanov E. An optimized disaggregation method for human lung tumors that preserves the phenotype and function of the immune cells. Journal of Leukocyte Biology. 2015;97:201–9. [PubMed: 25359999]
15. Lizotte PH, Jones RE, Keogh L, Ivanova E, Liu H, Awad MM, et al. Fine needle aspirate flow cytometric phenotyping characterizes immunosuppressive nature of the mesothelioma microenvironment. Sci Rep. 2016;6:31745. [PubMed: 27539742]
16. O'Brien S, Thomas RM, Wertheim GB, Zhang F, Shen H, Wells AD. Ikaros Imposes a Barrier to CD8+ T Cell Differentiation by Restricting Autocrine IL-2 Production. J Immunol. 2014;192:5118–29. [PubMed: 24778448]
17. Liu X, Ranganathan R, Jiang S, Fang C, Sun J, Kim S, et al. A Chimeric Switch-Receptor Targeting PD1 Augments the Efficacy of Second-Generation CAR T Cells in Advanced Solid Tumors. Cancer Res. 2016;76:1578–90. [PubMed: 26979791]
18. Riese MJ, Wang LCS, Moon EK, Joshi RP, Ranganathan A, June CH, et al. Enhanced Effector Responses in Activated CD8+ T Cells Deficient in Diacylglycerol Kinases. Cancer Res. 2013;73:3566–77. [PubMed: 23576561]
19. Simoni Y, Becht E, Fehlings M, Loh CY, Koo S-L, Teng KWW, et al. Bystander CD8+ T cells are abundant and phenotypically distinct in human tumour infiltrates. Nature. 2018;557:575–9. [PubMed: 29769722]
20. Djenidi F, Adam J, Goubar A, Durgeau A, Meurice G, de Montpreville V, et al. CD8 +CD103 +Tumor–Infiltrating Lymphocytes Are Tumor-Specific Tissue-Resident Memory T Cells and a Prognostic Factor for Survival in Lung Cancer Patients. J Immunol. 2015;194:3475–86. [PubMed: 25725111]
21. Kumar BV, Ma W, Miron M, Granot T, Guyer RS, Carpenter DJ, et al. Human Tissue-Resident Memory T Cells Are Defined by Core Transcriptional and Functional Signatures in Lymphoid and Mucosal Sites. Cell Rep. 2017;20:2921–34. [PubMed: 28930685]
22. Mueller SN, Mackay LK. Tissue-resident memory T cells: local specialists in immune defence. Nat Rev Immunol. 2016;16:79–89. [PubMed: 26688350]
23. Paley MA, Kroy DC, Odorizzi PM, Johnnidis JB, Dolfi DV, Barnett BE, et al. Progenitor and terminal subsets of CD8+ T cells cooperate to contain chronic viral infection. Science. 2012;338:1220–5. [PubMed: 23197535]
24. Buggert M, Tauriainen J, Yamamoto T. T-bet and Eomes are differentially linked to the exhausted phenotype of CD8+ T cells in HIV infection. PLoS Pathog. 2014;10:e1004251 [PubMed: 25032686]

25. Tauriainen J, Scharf L, Frederiksen J, Naji A, Ljunggren H-G, Sönnerborg A, et al. Perturbed CD8+ T cell TIGIT/CD226/PVR axis despite early initiation of antiretroviral treatment in HIV infected individuals. Sci Rep. 2017;7:40354. [PubMed: 28084312]
26. Twyman-Saint Victor C, Rech AJ, Maity A, Rengan R, Pauken KE, Stelekati E, et al. Radiation and dual checkpoint blockade activate non-redundant immune mechanisms in cancer. Nature. 2015;520:373–7. [PubMed: 25754329]
27. Huang AC, Postow MA, Orlowski RJ, Mick R, Bengsch B, Manne S, et al. T-cell invigoration to tumour burden ratio associated with anti-PD-1 response. Nature. 2017;545:60–5. [PubMed: 28397821]
28. Timperi E, Focaccetti C, Gallerano D, Panetta M, Spada S, Gallo E, et al. IL-18 receptor marks functional CD8(+) T cells in non-small cell lung cancer. Oncoimmunology. 2017;6:e1328337. [PubMed: 28811967]
29. Amir E-AD, Davis KL, Tadmor MD, Simonds EF, Levine JH, Bendall SC, et al. viSNE enables visualization of high dimensional single-cell data and reveals phenotypic heterogeneity of leukemia. Nat Biotechnol. 2013;31:545–52. [PubMed: 23685480]
30. Moon EK, Wang L-CS, Dolfi DV, Wilson CB, Ranganathan R, Sun J, et al. Multifactorial T cell Hypofunction That is Reversible Can Limit the Efficacy of Chimeric Antibody Receptor-transduced Human T cells in Solid Tumors. Clinical Cancer Research. 2014;20: 4262–73. [PubMed: 24919573]
31. Prinz PU, Mendler AN, Masouris I, Durner L, Oberneder R, Noessner E. High DGK- and Disabled MAPK Pathways Cause Dysfunction of Human Tumor-Infiltrating CD8+ T Cells That Is Reversible by Pharmacologic Intervention. J Immunol. 2012;188:5990–6000. [PubMed: 22573804]
32. Wang S-F, Fouquet S, Chapon M, Salmon H, Regnier F, Labroquère K, et al. Early T Cell Signalling Is Reversibly Altered in PD-1+ T Lymphocytes Infiltrating Human Tumors. PLoS ONE. 2011;6:e17621. [PubMed: 21408177]
33. Fourcade J, Sun Z, Pagliano O, Guillaume P, Luescher IF, Sander C, et al. CD8+ T Cells Specific for Tumor Antigens Can Be Rendered Dysfunctional by the Tumor Microenvironment through Upregulation of the Inhibitory Receptors BTLA and PD-1. Cancer Res. 2012;72:887–96. [PubMed: 22205715]
34. Frey AB. Suppression of T cell responses in the tumor microenvironment. Vaccine 2015;33:7393–7400. [PubMed: 26403368]
35. Kargl J, Busch SE, Yang GHY, Kim K-H, Hanke ML, Metz HE, et al. Neutrophils dominate the immune cell composition in non-small cell lung cancer. Nat Comms. 2017;8:14381.
36. Wherry EJ, Kurachi M. Molecular and cellular insights into T cell exhaustion. Nat Rev Immunol. 2015;15:486–99. [PubMed: 26205583]
37. Wherry EJ. T cell exhaustion. Nat Immunol. 2011;131:492–9.
38. Thommen DS, Koelzer VH, Herzig P, Roller A, Trefny M, Dimeloe S, et al. A transcriptionally and functionally distinct PD-1. Nat Med. 2018;7:994–1004.
39. Duraiswamy J, Ibegbu CC, Masopust D, Miller JD, Araki K, Doho GH, et al. Phenotype, function, and gene expression profiles of programmed death-1(hi) CD8 T cells in healthy human adults. J Immunol. 2011;186:4200–12. [PubMed: 21383243]
40. Baitsch L, Legat A, Barba L, Fuertes Marraco SA, Rivals J-P, Baumgaertner P, et al. Extended Co-Expression of Inhibitory Receptors by Human CD8 T-Cells Depending on Differentiation, Antigen-Specificity and Anatomical Localization. Ashour HM, editor. PLoS ONE. 2012;7:e30852. [PubMed: 22347406]
41. Thome JJC, Bickham KL, Ohmura Y, Kubota M, Matsuoka N, Gordon C, et al. Early-life compartmentalization of human T cell differentiation and regulatory function in mucosal and lymphoid tissues. Nat Med. 2016;22:72–7. [PubMed: 26657141]
42. Thome JJC, Farber DL. Emerging concepts in tissue-resident T cells: lessons from humans. Trends in Immunology. 2015;36:428–35. [PubMed: 26072286]
43. Doering TA, Crawford A, Angelosanto JM, Paley MA, Ziegler CG, Wherry EJ. Network analysis reveals centrally connected genes and pathways involved in CD8+ T cell exhaustion versus memory. Immunity. 2012;37:1130–44. [PubMed: 23159438]

44. Intlekofer AM, Takemoto N, Wherry EJ, Longworth SA, Northrup JT, Palanivel VR, et al. Effector and memory CD8+ T cell fate coupled by T-bet and eomesodermin. Nat Immunol. 2005;6:1236–44. [PubMed: 16273099]

45. Scheper W, Kelderman S, Fanchi LF, Linnemann C, Bendle G, de Rooij MAJ, et al. Low and variable tumor reactivity of the intratumoral TCR repertoire in human cancers. Nat Med. 2019;25:89–94. [PubMed: 30510250]

46. Li J, Lee Y, Li Y, Jiang Y, Lu H, Zang W, et al. Co-inhibitory Molecule B7 Superfamily Member 1 Expressed by Tumor-Infiltrating Myeloid Cells Induces Dysfunction of Anti-tumor CD8. Immunity. 2018;48:1–20. [PubMed: 29343431]

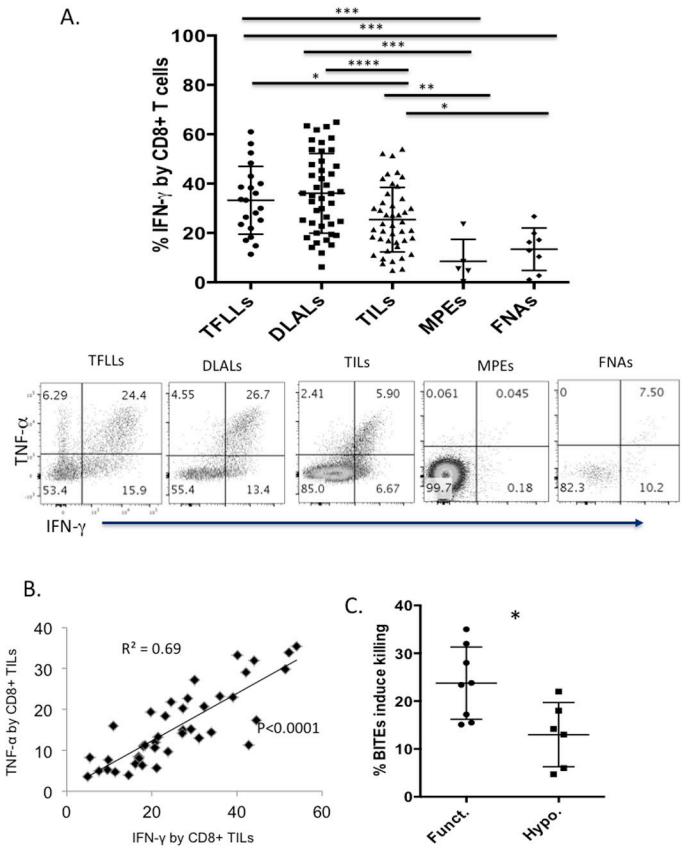

Figure 1: TCR stimulated early stage NSCLC CD8$^+$ TILs are functionally heterogeneous.

(**A**) Percent of CD8$^+$ T cells making intracellular IFNγ after overnight TCR stimulation of tumor free lungs (TFLLs) (n=21), lung tissue distant from the tumor (DLALs (n=44), tumor-infiltrating lymphocytes (TILs) (n=44), Malignant lung cancer pleural effusions (MPEs, n=5) and Fine Needle Aspirates of advanced lung cancer (FNAs, n=8). Dotted line marks one standard deviation below the TFLL mean. Representative CD8$^+$ TNFα$^+$ and IFNγ$^+$ flow plots from each tissue are depicted (bottom).

(**B**) Correlation of percent CD8$^+$ TILs making TNFα and IFNγ following overnight TCR stimulation (n=41). r^2= 0.69 by linear regression with a p value of <0.0001.

(**C**) Cytolytic activity of Functional (Funct) and Hypofunctional (Hypo) TILs (n=14), via the BiTE assay.

Parenthesis represents independent experimental assay repeats.

Note: * p<0.05, **p<0.01, ***p<0.001 and **** p<0.0001; n.s.-not significant

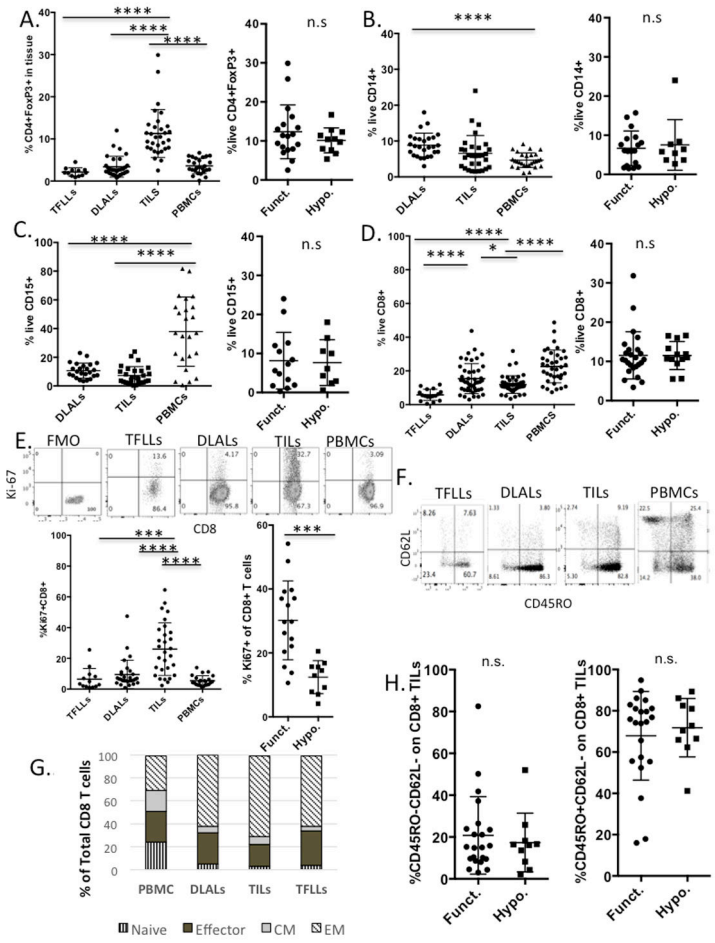

Figure 2: TIL functional heterogeneity is not associated with TME cell types or T-cell differentiation state, but with proliferation

(**A**) Left: $CD4^+FoxP3^+$ Regulatory T cells as a percentage of live cells in tumor digest in TFLLs (n=12), DLALs (n=31), TILs (n=31), and PBMCs (n=26); Right: Percentage of Tregs in functional vs hypofunctional TILs.

(**B**) Left: Monocytic cells ($CD14^+$) as a percentage of the live cells in tumor digest in DLALs, TILs, and PBMC. Right: $CD14^+$ percentage in functional vs hypofunctional TILs.

(**C**) Left: Neutrophilic cells ($CD15^+$) as a percentage of the live cells in tumor digest in DLALs, TILs, and PBMC. Right panel: $CD15^+$ percentage in functional vs hypofunctional TILs.

(D) Left: $CD8^+$ T cells plotted as a percentage of the live cells in tumor digest in TFLLs (n=17), DLALs (n=44), TILs (n=44) and PBMCs (n=40); Right: $CD8^+$ T cells percentage in functional vs hypofunctional TILs.

(**E**) Top: Representative flow plots of Ki-67 vs CD8 from control and patient samples. Left: $CD8^+$ T cell percentage expressing Ki-67 from TFLLs (n=13), DLALs (n=29), TILs(n=29) and PBMCs (n=23). Right: $CD8^+$ T percentage expressing Ki-67 cells in functional vs hypofunctional TILs.

(**F**) $CD8^+$ T-cell differentiation as shown in representative dot plot.

(**G**) $CD8^+$ T-cell Naïve, Effector, Central Memory, and Effector Memory frequencies were tabulated in PBMCs, DLALs, TILS and TFLLs.
(**H**) Effector (left) and Effector Memory $CD8^+$ T-cell frequencies (right) were compared in functional vs. hypofunctional TILs.
Parenthesis highlights independent flow staining repeats.
Note: * $p<0.05$, ***$p<0.001$, **** $p<0.0001$ and n.s. is not significant.

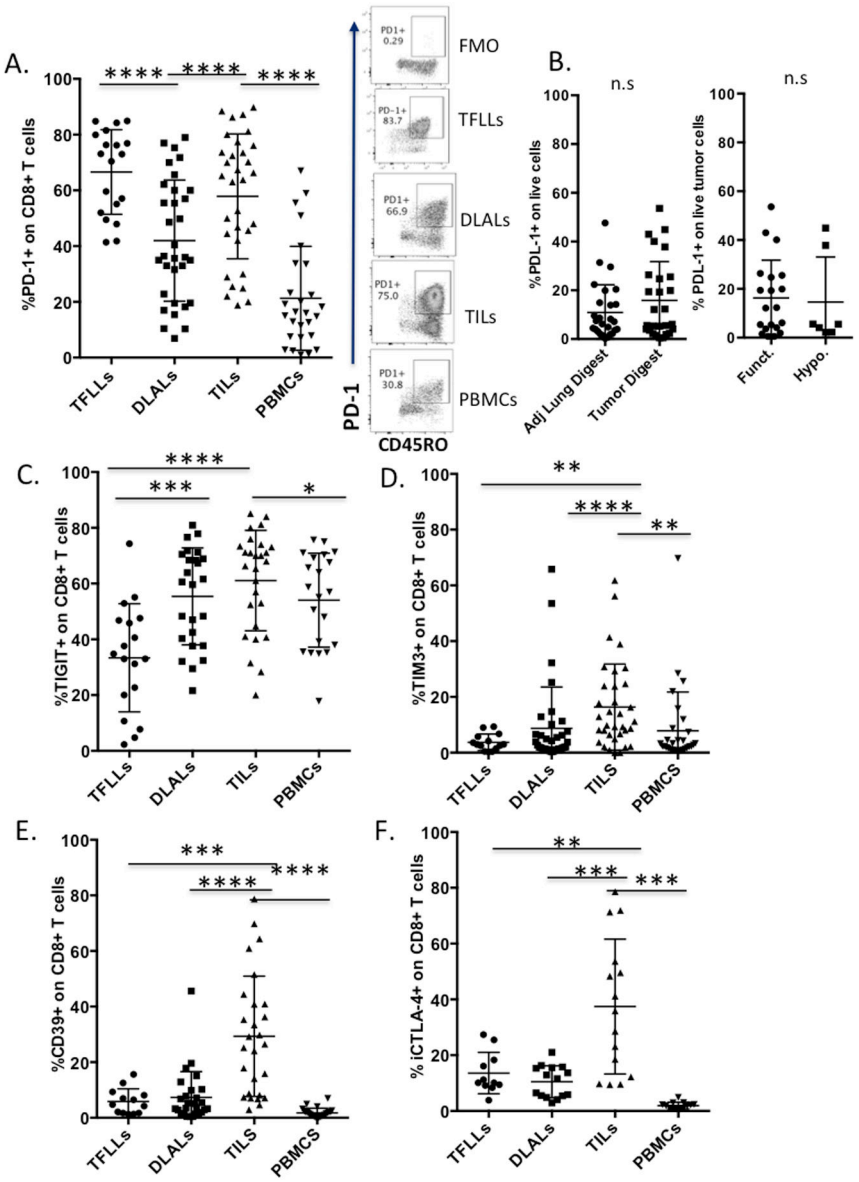

Figure 3: Tissue and PBMC lymphocyte inhibitory receptor expression is heterogeneous

(**A**) Left: Percentage of $CD8^{+}PD\text{-}1^{+}$ cells in TFLLs (n=19), DLALs (n=32), TILs (n=32) and PMBCs (n=27). Right: Representative flow plots of controls, TFLLs, DLALs, TILS and PBMCs for PD-1 and CD45RO on $CD8^{+}$ T cells.

(B) Percentage of live $CD3^{-}$ $PD\text{-}L1^{+}$ from adjacent distant lung (n=27) and tumor digests(n=27). Right : Percentage of $CD3^{-}$ $PD\text{-}L1^{+}$ cells in functional vs hypofunctional TILs (n=27).

(**C**) Percentage of $CD8^{+}TIGIT^{+}$ in TFLLs (n=18), DLALs (n=25), TILs (n=27) and PMBCs (n=21).

(**D**) Percentage of $CD8^{+}TIM3^{+}$ in TFLLs (n=14), DLALs (n=34), TILs (n=34) and PMBCs (n=30).

(**E**) Percentage of $CD8^+CD39^+$ in TFLLs (n=13), DLALs (n=27), TILs (n=27) and PMBCs (n=24).

(**F**) Percentage of $CD8^+$ cells expressing intracellular CTLA-4 in TFLLs (n=11), DLALs (n=15), TILs (n=15) and PBMCs (n=13).

Parenthesis represents independent flow staining repeats.

p<0.01,*p<0.001,****p<0.0001

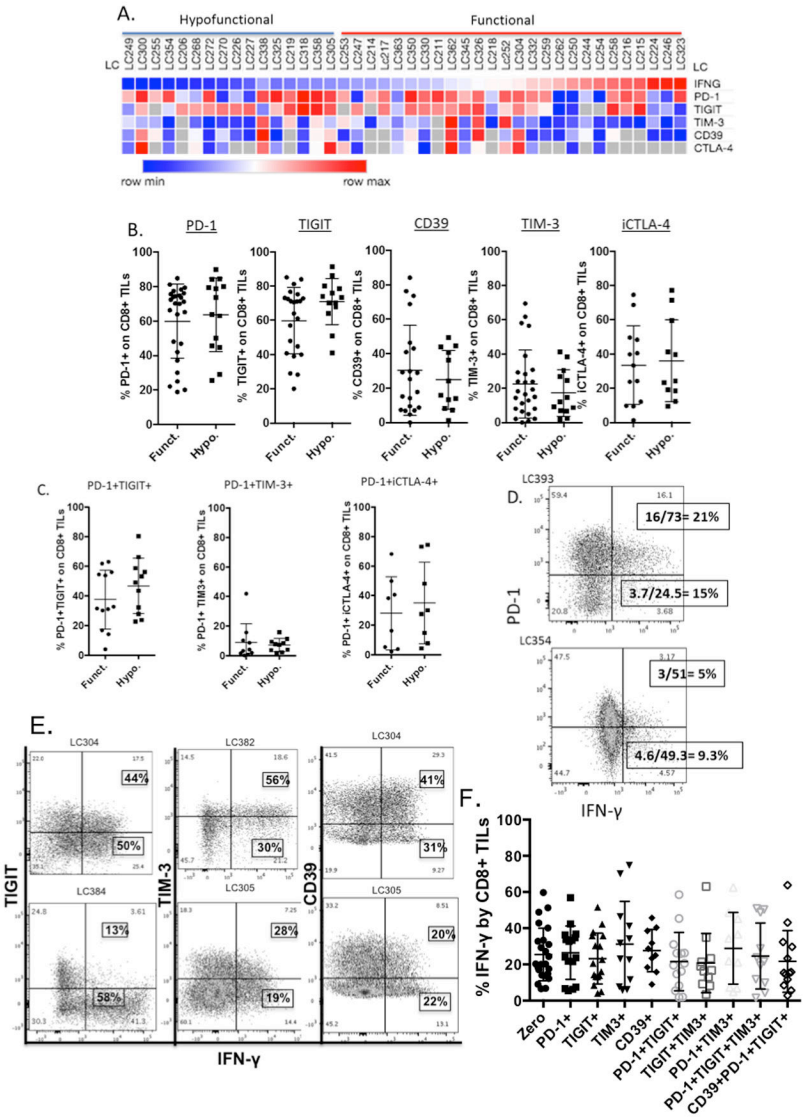

Figure 4: TIL function is not associated with inhibitory receptor expression

(A) Heatmap associations of relative expression of IFNγ production and inhibitory receptor frequencies (rows) for individual patient $CD8^+$ TILs (columns). Red-maximum; blue-minimum, grey-no values. Data were not transformed.

(B) The percentage of $CD8^+$ TILs expressing PD-1, TIGIT, CD39, TIM-3 and intracellular CTLA-4 was compared in functional (>19.3%) and hypofunctional (<19.3%) cases.

(C) The percentage of $CD8^+$ TILs expressing $PD\text{-}1^+TIGIT^+$, $PD\text{-}1^+TIM\text{-}3^+$, $PD\text{-}1^+iCTLA\text{-}4^+$ combinations were compared in functional and hypofunctional cases.

(D) Representative single cell analyses showing IFNγ expression (x-axis) versus PD1 expression (y axis) for two cases. The boxes depict the percentage of $PD\text{-}1^+$ $IFN\gamma^+$ (top) or $PD\text{-}1^-$ $IFN\gamma^+$ (bottom).

(E) Representative single cell analyses showing IFNγ expression (x-axis) versus TIGIT, TIM3 and CD39 expression (y axis) for four cases. The boxes depict the percentage of $TIGIT^+$ $IFN\gamma^+$, $TIM3^+$ $IFN\gamma^+$ or $CD39^+IFN\gamma^+$ cells.

(F) The percentage of $CD8^+$ TILs cells producing IFN**γ** based on their IR expression is plotted. Flow staining was performed individually for the TFLLs, and concurrently for the PBMCs, DLALs and TILS from each respective patient.
*p<0.05, ***p<0.001.

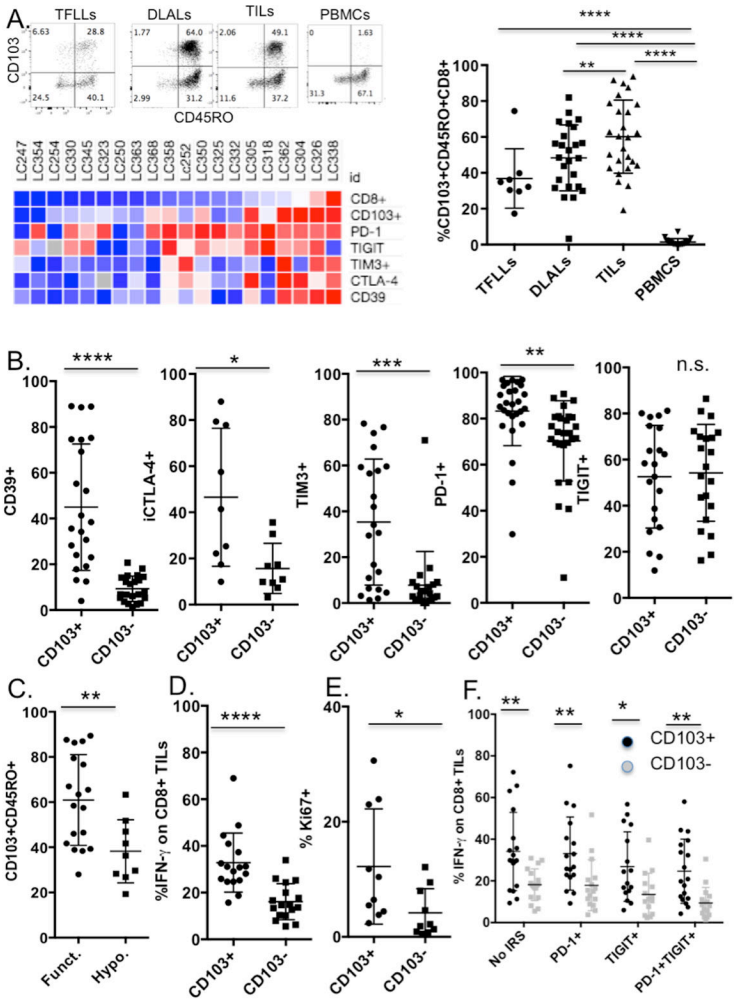

Figure 5: CD103$^+$ CD45RO$^+$ CD8$^+$ TILs are the main source of IFNγ

(A) Left upper panel: Tissue resident memory cells (T_{RM}s) were identified (upper right quadrants) as CD8$^+$CD103$^+$ RO$^+$ cells in TFLLs, DLALs, TILs, and PBMCs.

Right : The T_{RM} frequency is plotted for TFLLs (n=8), DLALs (n=25), TILs (n=26) and PBMCs (n=18).

Left lower panel: Heatmap associations of the relative expression of CD8$^+$ TIL frequency, CD103, and IRs (rows) expression on individual CD8$^+$ TILs (columns). Red-maximum, blue-minimum, grey-no values. Data are not transformed.

(**B**) IR expression (CD39, iCTLA-4, TIM-3, PD-1, and TIGIT) on CD8$^+$CD103$^+$ versus CD8$^+$CD103$^-$ TILs.

(**C**) Percentage of CD8$^+$CD45RO$^+$ cells expressing CD103 in functional vs hypofunctional TILs.

(**D**) Re-stimulated CD103$^+$ CD8$^+$ were compared to CD103$^-$ CD8$^+$TILs for their IFNγ production.

(**E**) Baseline Ki-67 expression on CD103$^+$ CD8$^+$ was compared to CD103$^-$ CD8$^+$ TILs.

(**F**) By single cell analysis, the percentage of $CD8^+$ TILs cells producing IFN**γ** based on their IR expression and CD103 status [$CD103^+$ (black) and $CD103^-$ (grey)] is plotted. One-Way ANOVA compared $CD103^+$ IR^- vs. $CD103^+$ IR^+ and were non-significant.
Note: * $p<0.05$, ** $p<0.01$, *** $p<0.001$ and **** $p<0.0001$

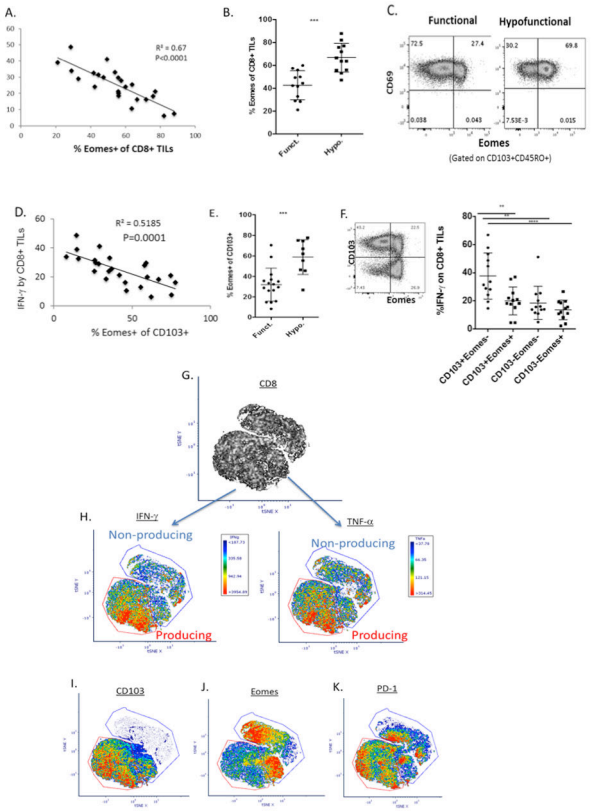

Figure 6: Eomes expression in TIL CD103$^+$ Tissue Resident Memory Cells is associated with hypofunction

(A) The percentage of CD8$^+$ TILs producing IFNγ versus their EOMES expression was plotted and a negative correlation was found.

(B) The CD8$^+$Eomes$^+$ percentage was compared between functional and hypofunctional cases.

(C) Representative flow plots of Eomes and CD69 expression on CD103$^+$ CD45RO$^+$ CD8$^+$ T_{RM}s for a functional and hypofunctional case illustrating higher Eomes expression with hypofunction.

(D) For each patient, the percentage of CD8$^+$ TILs producing IFNγ versus the percentage of CD103$^+$ CD8$^+$ TILs expressing EOMES was plotted. A negative correlation was found.

(E) The Eomes percentage in CD103$^+$ CD8$^+$ TILs were compared between functional and hypofunctional cases.

(F) Left: Representative tracing of CD103 versus EOMES expression. Right: The graph represents the IFNγ percentage by CD103$^+$Eomes$^-$, CD103$^+$Eomes$^+$, CD103$^-$Eomes$^-$, and CD103$^-$Eomes$^+$ CD8$^+$ TILs from left panel (n=12). One-Way ANOVA test was applied.

(G) CD8+ T cell ViSNE analysis of a functional TIL case.

(H) IFNγ (left panel) and TNFα (right panel) expression by each cell [red= high, blue = low expression] were superimposed on CD8 map revealing "cytokine producing" (Red circle) and "cytokine non-producing" (Blue Circle) regions.

(I) CD103 expression (red-high; blue-low) is overlaid.

(J) Eomes expression (red-high; blue-low) is overlaid.

(K) PD-1 expression (red-high; blue-low) is overlaid.

* $p<0.05$, ** $p<0.01$

Table 1:

Patient Clinical and Demographic Data

	NSCLC Patients (n=44)		Fine Needle Aspirates (n=8)		Malignant Pleural Effusion (n=5)		Tumor Free Lung Donors (n=21)	
	Number	**%**	**Number**	**%**	**Number**	**%**	**Number**	**%**
Median Age (range)	67 (50–84)		73(60–88)		68(59–75)		63(28–72)	
Gender								
Male	17	39	4	50	2	40	15	71
Female	27	61	4	50	3	60	8	28
Race								
White or Other	36	82	5	62	2	40	19	90
Black	8	18	3	38	3	60	2	10
Smoking								
Current	4	9	NA				1	5
Former	29	66	7	88	3	60	10	47
Never	11	25	1	12	2	40	10	47
Histology								
Adenocarcinoma	34	77	6	75	5	100		
Squamous	8	18	2	25				
Large Cell Neuroendocrine	2	5						
Epithelioid								
Pleomorphic								
Disease Stage								
I	22	50	1	12				
II	13	30	1	13				
III	9	20	2	25				
IV			4	50	5	100		
Tumor Size								
< 3cm	21	48	1	12				
≥ 3cm	23	52	7	88				
Cause of Death								
CVA (incl. stroke)							12	57
Anoxia							7	33
Head Trauma							2	9
Ischemia Time							7hrs (5–20)	